

Low-energy nuclear spin excitations in NdMg₃ and NdCo₂

Tapan Chatterji,¹ G. J. Schneider,² and R. M. Galera³

¹Institut Laue-Langevin, B.P. 156, 38042 Grenoble Cedex, France

²JCNS, Institut für Festkörperforschung, Forschungszentrum Jülich, 52425 Jülich, Germany

³Institut Néel, CNRS, B.P. 166, 38042 Grenoble, France

(Received 15 May 2008; published 22 July 2008)

We investigated the low-energy excitations in NdMg₃ and NdCo₂ in the μeV range by a backscattering neutron spectrometer. The energy scans on polycrystalline NdMg₃ and NdCo₂ samples revealed inelastic peaks at $E=1.70\pm 0.01\ \mu\text{eV}$ and $3.37\pm 0.01\ \mu\text{eV}$, respectively, at $T=2\ \text{K}$ on both energy gain and loss sides. The inelastic peaks move gradually toward lower energy with increasing temperature and finally merge with the elastic peak at the electronic magnetic ordering temperature $T_N\approx 6\ \text{K}$ and $T_C\approx 100\ \text{K}$, respectively. We interpret the inelastic peaks to be due to the transition between hyperfine-split nuclear levels of the ¹⁴³Nd and ¹⁴⁵Nd isotopes with spin $I=7/2$.

DOI: 10.1103/PhysRevB.78.012411

PACS number(s): 75.25.+z

With the advent of high resolution backscattering neutron spectrometer, Heidemann and coworkers¹⁻⁷ investigated the hyperfine fields in Co- and V-based compounds. The hyperfine splitting lies typically in the energy range of a few μeV . The inelastic spin-flip scattering of neutrons from the nuclear spins can yield this information, provided the neutron spectrometer has the required resolution of about μeV and also the incoherent scattering of the nucleus is strong enough. It was established that the hyperfine field produced at the nucleus is roughly but not exactly proportional to the electronic magnetic moment of the 3d shell—an expected result. Heidemann¹ worked out the double differential cross-section of this scattering process. The process can be summarized as follows: If neutrons with spin s are scattered from nuclei with spins \mathbf{I} , the probability that their spins will be flipped is $2/3$. The nucleus at which the neutron is scattered with a spin-flip changes its magnetic quantum number M to $M\pm 1$ due to the conservation of the angular momentum. If the nuclear ground state is split up into different energy levels E_M due to the hyperfine magnetic field or an electric quadrupole interaction, then the neutron spin-flip produces a change of the ground state energy $\Delta E=E_M-E_{M\pm 1}$. This energy change is transferred to the scattered neutron. The double differential scattering cross-section¹ is given by the following expressions:

$$\left(\frac{d^2\sigma}{d\Omega d\omega}\right)_{\text{inc}}^0 = \overline{\left(\alpha^2 - \bar{\alpha}^2 + \frac{1}{3}\alpha'^2 I(I+1)\right)} e^{-2W(k)} \delta(\hbar\omega), \quad (1)$$

$$\left(\frac{d^2\sigma}{d\Omega d\omega}\right)_{\text{inc}}^{\pm} = \frac{1}{3}\overline{\alpha'^2 I(I+1)} \sqrt{1 \pm \frac{\Delta E}{E_0}} e^{-2W(k)} \delta(\hbar\omega \mp \Delta E), \quad (2)$$

where α and α' are coherent and spin-incoherent scattering lengths, $W(k)$ is the Debye-Waller factor, E_0 is the incident neutron energy, and δ is the Dirac delta function. If the sample contains one type of isotope, then $\alpha^2 - \bar{\alpha}^2$ is zero. Also $\sqrt{1 \pm \frac{\Delta E}{E_0}} \approx 1$ because ΔE is usually much less than the incident neutron energy E_0 . In this case, $2/3$ of incoherent scattering will be spin-flip scattering. One therefore expects a central elastic peak and two inelastic peaks of approximately

equal intensities. Obviously the measured spectrum will be a convolution of the cross-section given in Eqs. (1) and (2) with the resolution function of the spectrometer.

The Nd has the natural abundances of 12.18% and 8.29% of ¹⁴³Nd and ¹⁴⁵Nd isotopes, respectively. Both of these isotopes have a nuclear spin of $I=7/2$ and their incoherent scattering cross-sections⁸ are relatively large, 55 ± 7 and 5 ± 5 barn for ¹⁴³Nd and ¹⁴⁵Nd, respectively. Therefore Nd-based compounds are very much suitable for such studies. We investigated the low-energy nuclear spin excitations on Nd metal and several Nd-based compounds⁹⁻¹² by inelastic neutron scattering, and found that the energy of the excitations in these compounds are approximately proportional to the ordered 4f electronic magnetic moment that is usually much reduced from the free ion value of $3.27\mu_B$ due to the crystal-field effects. Recently Przenioslo *et al.*¹³ investigated nuclear ordering and excitations in NdFeO₃ and found similar results.

In order to check the validity of the linear relationship between the ordered electronic magnetic moment and the energy of excitations or the hyperfine splitting, we investigated the low-energy excitations in intermetallic Nd compounds; NdMg₃ and NdCo₂ at low temperatures. NdMg₃ crystallizes with the DO₃-type crystal structure with the $Fm\bar{3}m$ space group. The Nd atoms in NdMn₃ form a fcc sublattice. The lattice constant of NdMg₃ at room temperature is $7.39\pm 0.02\ \text{\AA}$. Neutron diffraction¹⁴ investigations have established that NdMg₃ undergoes an antiferromagnetic transition at $T_N\approx 6\ \text{K}$ with the propagation vector $\mathbf{k}=(\frac{1}{2}, \frac{1}{2}, \frac{1}{2})$ and has a type-III magnetic structure. The ferromagnetic (111) layers are stacked antiferromagnetically along the [111] axis. The magnetic moments make an angle ϕ between 70 to 90° with the [111] axis.¹⁴ The ordered magnetic moment per Nd ion was determined to be $\mu=1.30\pm 0.04\mu_B$. It should however be noted that it is not possible to distinguish between possible single- \mathbf{k} , double- \mathbf{k} , and triple- \mathbf{k} structures from neutron powder diffraction intensities without applying uniaxial stress or magnetic field. The other intermetallic compound NdCo₂ crystallizes with the well-known Laves phase structure with the space group $Fd\bar{3}m$. The lattice parameter at $T=200\ \text{K}$ is $a=7.2914\pm 0.0002\ \text{\AA}$ (Ref. 15). With decreasing temperature, NdCo₂

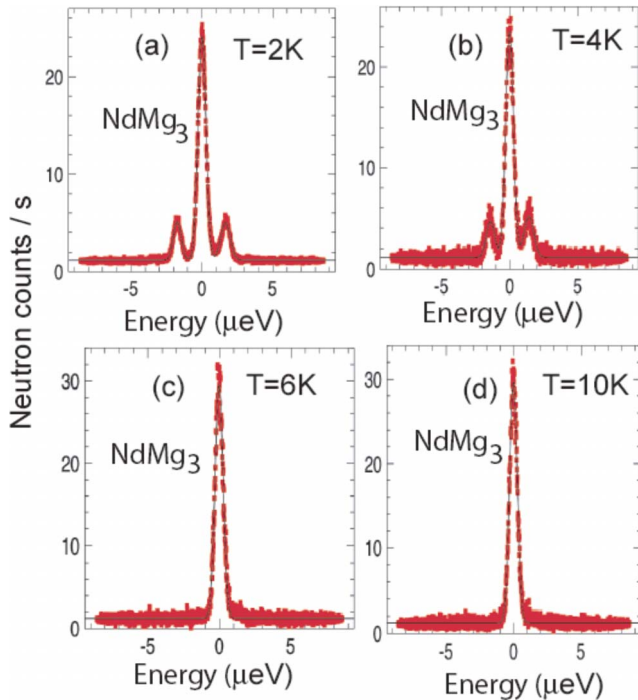


FIG. 1. (Color online) Typical energy spectra of NdMg_3 at several temperatures. The continuous curves are the results of the fit of the data with three Gaussian functions.

exhibits a tetragonal distortion ($I4_1/amd$) below the ferromagnetic Curie temperature $T_C \approx 100$ K and an orthorhombic distortion ($Fddd$) below $T=42$ K. The neutron diffraction investigation¹⁵ gave a magnetic moment of Nd-ion $2.80\mu_B$, close to its free trivalent value, and the Co moment of $0.73\mu_B$.

We performed inelastic neutron scattering experiments on polycrystalline NdMg_3 at low temperatures by using the high resolution backscattering neutron spectrometer SPHERES of the Jülich Centre for Neutron Science located at the FRM reactor in Munich (FRMII). The wave length of the incident neutrons was $\lambda=6.271$ Å. About 20 g of polycrystalline samples of NdMg_3 was placed in a flat aluminum sample holder and was fixed to the cold tip of a cryostat. We observed inelastic signals in NdMg_3 at energy $E=1.70 \pm 0.01$ μeV on both energy gain and loss sides at $T=2$ K. The energy of the inelastic signal decreases continuously as the temperature is increased and finally merges with central elastic peak at $T_N \approx 6$ K. Figure 1 shows typical energy spectra of NdMg_3 at several temperatures. The spectra is the result of averaging the counts of the individual detectors placed at different scattering angles. The continuous curves are the results of the fit of the data with three Gaussian functions. The inelastic signals have resolution-limited widths at least at low temperatures. At higher temperatures where the inelastic peaks are very close to the central elastic peak, it was difficult to determine the widths by the fitting procedure and had to be constrained. There are two ^{143}Nd and ^{145}Nd isotopes with a nuclear spin of $I=7/2$ in NdMg_3 . So one might expect two inelastic lines corresponding to these two isotopes. But experimentally, only one resolution-limited inelastic line is observed. This is also the case in

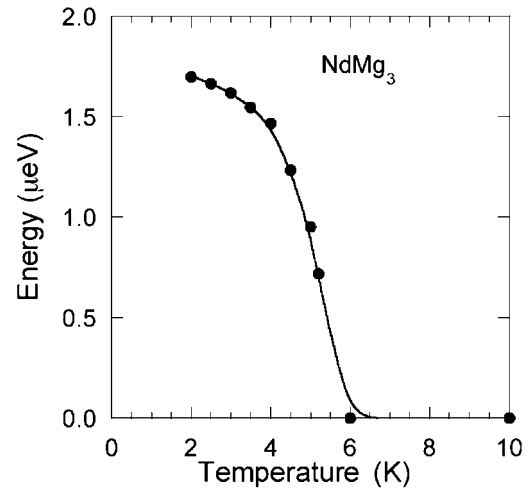


FIG. 2. Temperature variation of the energy of the inelastic peak of NdMg_3 . The continuous line is just a guide to the eye.

Nd_2CuO_4 (Ref. 9), NdCu_2 (Ref. 11), and NdGaO_3 (Ref. 12). Two inelastic lines were seen in Nd metal,¹⁰ which we interpreted as due to the two different crystallographic hexagonal and cubic sites of the dhcp structure of Nd and are not due to two different Nd isotopes. The reason for only one inelastic signal in Nd_2CuO_4 , NdCu_2 , and NdGaO_3 is probably that ^{145}Nd isotope contributes little to the scattering due to the small incoherent scattering cross-section of ^{145}Nd (5 ± 5 barn). Figure 2 shows the temperature dependence of the energy of the inelastic peak. The energy of the inelastic peak decreases continuously and becomes zero at $T_N \approx 6$ K. It is to be noted that the intensity of the inelastic peak at $T=2$ K is about one fifth of that of the elastic peak. One expects from Eqs. (1) and (2) that the inelastic peaks have the same intensities as that of the elastic peak. The incoherent scattering cross-sections of Mg is 0.077 barn contribute to the intensity of the incoherent elastic peak. The remaining possibilities are the contributions from the sample holder and coherent Bragg peaks. The sample holder consists of Al, which has a very small incoherent scattering cross-section of 0.0082 barn. This is probably the origin of the extra intensity in the elastic peak. Heideman *et al.*^{2,3,6} observed similar excess of intensity at the elastic peak in several experiments on vanadium oxides.

We did similar measurements on NdCo_2 that orders ferromagnetically¹⁵ at about $T_C=100$ K. Two inelastic peaks were observed at about $E=3.4$ μeV $T=2$ K on both energy gain and loss sides. We identify these peaks to be due to the hyperfine splitting of ^{143}Nd nucleus. There should be a hyperfine splitting of the Co nuclear levels as well. However, due to the small ordered moment of $0.73\mu_B$ of the Co atom, the inelastic peak should have a small energy. Heidemann⁴ found a hyperfine splitting of about $0.5\mu\text{eV}/\mu_B$ in amorphous ferromagnetic Co-P alloys. From this, we estimate the hyperfine splitting of $0.37\mu\text{eV}$ in NdCo_2 . So the inelastic peak for the hyperfine splitting of the Co should be very close to the elastic peak due to the finite instrumental resolution (full at half-maximum FWHM= $0.65\mu\text{eV}$), and therefore has not been resolved. A small intensity is observed on the right side of the elastic peak at about 1 μeV at all tem-

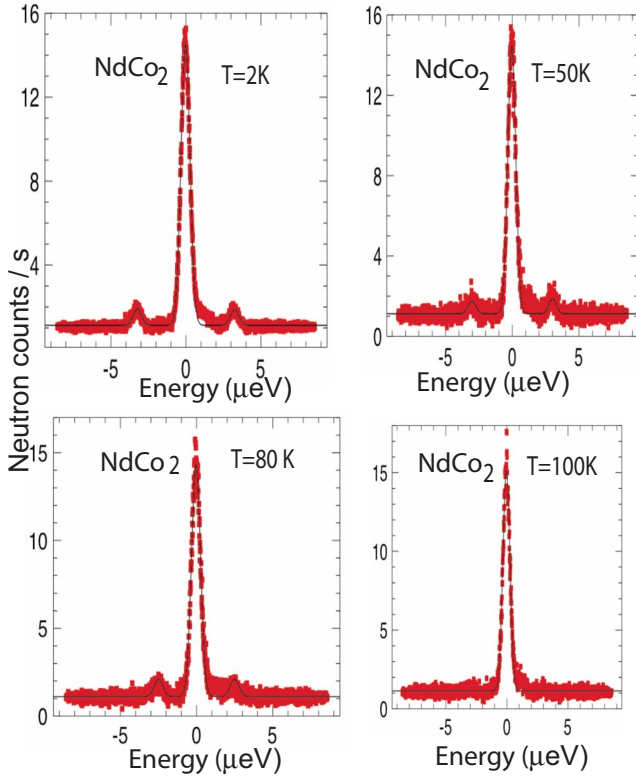


FIG. 3. (Color online) Typical energy spectra of NdCo₂ at several temperatures. The continuous curves are the results of the fit of the data with three Gaussian functions.

peratures. This may be due to the imperfect resolution function of the instrument but can as well be due to the presence of small amount of ferromagnetic Co impurity in the sample. The energy of the inelastic peaks decreases continuously as the temperature is increased and finally merges with the central elastic peak at $T_C \approx 100$ K. Such as in the case of NdMg₃, the inelastic signals in NdCo₂ also have resolution-limited widths. Figure 3 shows typical inelastic spectra of NdCo₂ at several temperatures. Figure 4 shows the temperature dependence of the energy of the inelastic peak. The en-

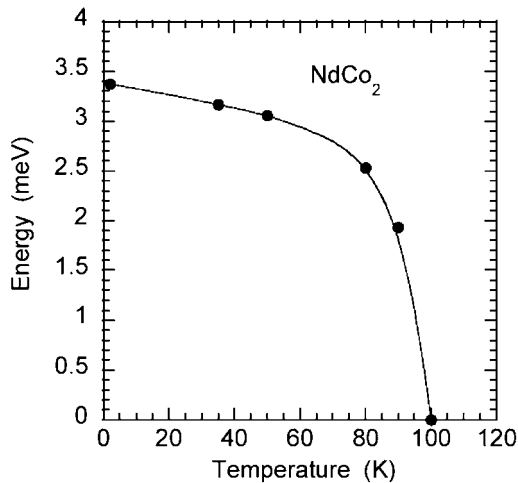


FIG. 4. Temperature variation of the energy of the inelastic peak of NdCo₂. The continuous line is just a guide to the eye.

ergy of the inelastic peak decreases continuously and becomes zero at $T_C \approx 100$ K.

The hyperfine magnetic field at the nucleus of Nd³⁺ ion in the ordered state in a Nd-based compound is caused by the open 4*f* shell, core polarization, and if the sample is metallic by conduction-electron polarization (CEP). The dominant contribution from the 4*f* shell can be written as^{16,17}

$$H_{4f} = 2\mu_B \langle J || N || J \rangle \langle r^{-3} \rangle_{\text{eff}} \langle J_z \rangle. \quad (3)$$

For the ⁴I_{9/2} ground state of Nd³⁺, the reduced matrix element $\langle J || N || J \rangle$ is 1.31. (Refs. 16 and 17). We take a mean value of $\langle r^{-3} \rangle_{\text{eff}} = 5.78$ a.u. for Nd³⁺. $\langle J_z \rangle$ is given by $\mu_z = g_L \mu_B \langle J_z \rangle$, and with $g_L = 8/11$ one calculates $H_{4f} = 129.3 \mu_z \text{T}$, where μ_z is the Nd³⁺ ionic moment. The contribution of core polarization is approximately given by $H_c = -90(g_L - 1)J$, which is 12.5 Tesla for Nd³⁺ in the ⁴I_{9/2} state. We assume that the contribution of the CEP is negligible. So one expects a hyperfine magnetic field of $H = H_{4f} + H_c = 116.8 \mu_z$ Tesla at the Nd nucleus. The hyperfine magnetic field at the Nd nucleus produces the splitting ΔE of $I = 7/2$ into eight equally spaced levels neglecting quadrupolar term given by

$$H = \frac{I \Delta E}{\mu \mu_N}, \quad (4)$$

where μ_N is the nuclear magneton, and μ is the number of nuclear magnetons which the nucleus possesses. From Eqs. (3) and (4) one expects the energy ΔE of the inelastic line to be proportional to the ordered Nd electronic magnetic moment. From Eq. (4) one can calculate the hyperfine field at the nucleus from the experimental value of ΔE determined by the inelastic neutron scattering, provided one knows the magnetic moment of the nucleus. The magnetic moments of ¹⁴³Nd and ¹⁴⁵Nd nuclei are tabulated by Bleaney¹⁷ to be -1.063 ± 0.005 and -0.654 ± 0.004 nuclear magnetons, respectively. We believe that in the inelastic neutron scattering, we mainly see the signal from ¹⁴³Nd. Therefore to calculate the hyperfine field from the experimental value of the splitting ΔE , we use the magnetic moment of -1.063 ± 0.005 nuclear magnetons in Eq. (4). The hyperfine field at the ¹⁴³Nd nucleus is calculated to be 156.2 and 309.8 Tesla for NdMg₃ and NdCo₂ by using the experimental values $\Delta E = 1.70 \pm 0.01 \mu\text{eV}$ and $\Delta E = 3.37 \pm 0.01 \mu\text{eV}$ at 2 K. The magnetic moments of ¹⁴³Nd and ¹⁴⁵Nd nuclei are given in Ref. 18 to be -1.208 and -0.744 nuclear magnetons, respectively. Using these values, we recalculate the hyperfine field at the ¹⁴³Nd nucleus from the measured ΔE to be 156.2 and 309.8 Tesla for NdMg₃, and NdCo₂, respectively.

Figure 5 shows a plot of energy of inelastic peaks in NdCuO₄ (Ref. 9), Nd metal,¹⁰ NdCu₂ (Ref. 11), NdGaO₃ (Ref. 12), NdMg₃, NdCo₂, and NdMnO₃ (Ref. 19) vs the corresponding electronic magnetic moment of Nd in these compounds, determined by the refinement of the magnetic structure using magnetic neutron diffraction intensities. The data lie approximately on a straight line showing that the hyperfine field at the nucleus is approximately proportional to the electronic magnetic moment. The slope of the linear fit of the data gives a value of $1.25 \pm 0.04 \mu\text{eV} / \mu_B$. It is to be

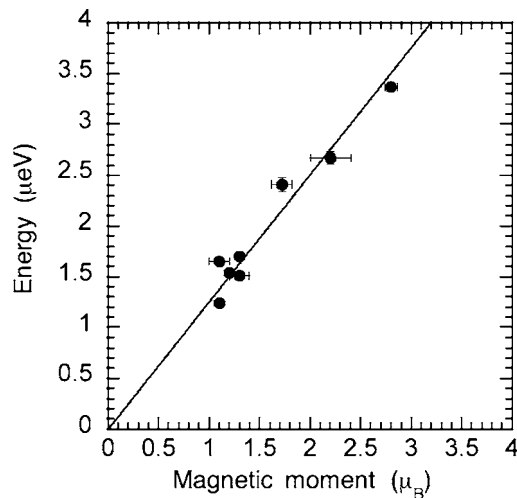


FIG. 5. Plot of energy of the inelastic signals in NdCuO₄, Nd metal, NdCu₂ and NdGaO₃, NdMg₃ and NdCo₂, NdMnO₃, and NdFeO₃ vs. the corresponding saturated electronic magnetic moment of Nd in these compounds at low temperatures.

noted that the data for the hyperfine splitting is rather accurate, whereas the magnetic moment determined by neutron diffraction has a large standard deviation and is dependent on the magnetic structure model. The magnetic structures are seldom determined unambiguously, and the magnetic moment determined from the refinement of a magnetic structure model is relatively uncertain. In such cases, the investigation of the low-energy excitations described here can be of additional help. This is especially true for the complex magnetic structures with two magnetic sublattices of which one sublattice contains Nd. Such complex magnetic structures, such as the parent compounds of Fe-based superconductors, colossal magnetoresistive manganites, and some multiferroic materials are currently under intense study.

We interpret the inelastic signal observed in NdMg₃ due to the excitations of the Nd-nuclear spin $I = \frac{7}{2}$ of the ¹⁴³Nd and ¹⁴⁵Nd isotopes. In a first approximation, one can consider these inelastic peaks to arise due to the transitions between the hyperfine-field-split nuclear levels. This is the single-nucleus effect. However, the nuclear spins are coupled through Suhl-Nakamura interaction.^{20,21} So one expects nuclear spin wave excitations (cooperative lattice effect) discussed by de Gennes *et al.*²² according to which the nuclear spin waves should have dispersions at a very small q . Word *et al.*²³ discussed the possibility of measuring nuclear spin waves by inelastic neutron scattering. Also, they have developed the differential scattering cross-section and scattered state polarization for the scattering of neutrons from systems described by Suhl-Nakamura Hamiltonian in the formalism of van Hove correlation function. In our experiment, due to the insufficient Q resolution of the backscattering spectrometer and also because of the polycrystalline sample used, we could not measure the expected dispersion of the nuclear spin waves. The dispersion of the nuclear spin waves can perhaps be measured on single crystals at very low temperatures by a neutron spin echo (NSE) spectrometer.

In conclusion, we have investigated the low-energy excitations in NdMg₃ and NdCo₂ by the backscattering neutron spectrometer. The present results together with our previous results on several Nd-based compounds have shown that the ordered electronic magnetic moment of Nd ion is linearly proportional to the energy of excitations or the hyperfine splitting. In case of complex magnetic structures with two magnetic sublattices, the present technique can give additional information about the ordered electronic magnetic moment or the order parameter.

We wish to thank H. Schneider and M. Prager for their help during the experiment.

¹A. Heidemann, Z. Phys. **238**, 208 (1970).

²A. Heidemann and B. Alefeld, *Neutron Inelastic Scattering* (International Atomic Energy Agency, Vienna, 1972).

³A. Heidemann, Phys. Status Solidi A **16**, K129 (1973).

⁴A. Heidemann, Z. Phys. B **20**, 385 (1975).

⁵A. Heidemann, D. Richter, and K. H. J. Buschow, Z. Phys. B **22**, 367 (1975).

⁶A. Heidemann, K. Kosuge, and S. Kachi, Phys. Status Solidi A **35**, 481 (1976).

⁷A. Heidemann, K. Kosuge, Y. Ueda, and S. Kachi, Phys. Status Solidi A **39**, K37 (1977).

⁸V. F. Sears, in *International Tables for Crystallography*, 2nd ed., edited by A. J. C. Wilson and E. Prince (Kluwer, Dordrecht, 1999), Vol. C, p. 445.

⁹T. Chatterji and B. Frick, Physica B (Amsterdam) **276-278**, 252 (2000).

¹⁰T. Chatterji and B. Frick, Appl. Phys. A: Mater. Sci. Process. **A74**, S652 (2002).

¹¹T. Chatterji and B. Frick, Physica B (Amsterdam) **350**, e111 (2004).

¹²T. Chatterji and B. Frick, Solid State Commun. **131**, 453 (2004).

¹³R. Przenioslo, I. Sosnowska, and B. Frick, J. Magn. Magn. Mater. **305**, 186 (2006).

¹⁴R. M. Galera, J. Pierre, and J. Pannetier, J. Phys. F: Met. Phys. **12**, 993 (1982).

¹⁵Z. W. Ouyang, F. W. Wang, Q. Huang, W. F. Liu, Y. Q. Xiao, J. W. Lynn, J. K. Liang, and G. H. Rao, Phys. Rev. B **71**, 064405 (2005).

¹⁶R. J. Elliot and K. W. H. Stevens, Proc. R. Soc. London, Ser. A **218**, 553 (1953).

¹⁷B. Bleaney, in *Magnetic Properties of Rare Earth Metals*, edited by R. J. Elliot (Plenum, New York, 1972).

¹⁸R. K. Harris, in *Encyclopedea of Nuclear Magnetic Resonance*, edited by D. M. Granty and R. K. Harris (Wiley, New York, 1996), Vol. 5.

¹⁹T. Chatterji, G. J. Schneider, and D. Bhattacharya (unpublished).

²⁰H. Suhl, Phys. Rev. **109**, 606 (1958).

²¹T. Nakamura, Prog. Theor. Phys. **20**, 542 (1958).

²²P. G. de Gennes, P. A. Pincus, F. Hartmann-Boutron, and J. M. Winter, Phys. Rev. **129**, 1105 (1963).

²³R. Word, A. Heidemann, and D. Richter, Z. Phys. B **28**, 23 (1977).